ICWE14
June 21-26, 2015 | Porto Alegre - Brazil
14th INTERNATIONAL CONFERENCE ON WIND ENGINEERING

Modeling night-time ventilation in Stanford's Y2E2 building

Catherine Gorlé[1,2], Asha Chigurupati[1], Gianluca Iaccarino[1]
[1]Department of Mechanical Engineering, Stanford University, Stanford, CA, USA
[2]Department of Civil Engineering and Engineering Mechanics, Columbia University, New York City, NY, USA
email: catherine.gorle@columbia.edu, ashac@stanford.edu, jops@stanford.edu

ABSTRACT: An important fraction of the energy consumption in buildings is related to controlling the indoor temperature. In moderate climates passive cooling by nighttime ventilation can result in significant energy savings, but modeling natural ventilation systems for design and performance predictions remains a challenging task. We investigate the predictive capability of a box model and a CFD simulation for modeling night-flush ventilation in the Y2E2 building on Stanford's campus. Both models consider a single atrium of the building and the predictions are compared to available temperature measurements.

The box model solves for the average air and building thermal mass temperatures, and represents heat sources and sinks as integral values. The uncertainty in the input parameters for the box model is propagated to the output using a non-intrusive polynomial chaos method. The mean result predicts a too fast cooling rate, but the maximum discrepancy with the measured data is limited to 0.6K, and the measurements are within the predicted 95%CI. The uncertainty in the results is mainly related to uncertainty in the infiltration flow rate, the initial thermal mass temperature, the internal heat source, and the heat transfer coefficient. The CFD simulation represents a much higher level of detail in the building model, but it also predicts a too high cooling rate. The maximum discrepancy between the average air temperature from the CFD model and the measurement was found to be 0.9K. The discharge coefficients computed from the CFD simulation depend on the floor and the time during the nightflush and vary from 1.1 to 0.15, which is outside of the range originally assumed in the box model UQ study. The average heat transfer coefficient computed from the simulations is around 2.8W/m^{2}K, which is within the range used by the box model.

KEY WORDS: Natural Ventilation, Computational Fluid Dynamics, Box Model, Uncertainty Quantification.

1 INTRODUCTION

Commercial and residential buildings account for ~40% of the energy consumption in the United States [1], and current studies do not project changes in the next two decades. Among the sources of energy use in buildings, an important fraction is consumed to control the indoor temperature through heating, ventilating or air conditioning. Significant energy savings can be achieved by implementing energy efficient strategies such as mixed-mode ventilation or passive ventilation. In moderate to cold climates passive cooling by nighttime ventilation is particularly interesting, because low nighttime temperatures allow cooling a building while it is unoccupied, and during the day the low temperature thermal mass provides a heat sink when temperatures rise. Northern California's climate has substantial potential for cooling using nighttime ventilation, and several recent buildings on Stanford's campus are therefore designed for night-flush cooling.

Even in favorable climates the design and performance prediction of a natural ventilation system remains a challenging task. Designers and engineers have access to a hierarchy of computational models, reflecting increasing levels of complexity in the representation of the physical processes involved. At the lowest level of complexity there are reduced order integral models (box models), which solve for the average temperature of the air and the building thermal mass, and represent heat sources and sinks using integral values. Building simulation tools such as EnergyPlus can incorporate considerably more detailed information on the building design and corresponding heat sources and sinks, and simplified airflow models are implemented to represent cooling from natural ventilation. Unfortunately realistic building layouts create a degree of complexity in the flow pattern that cannot be captured accurately using these basic models. Computational fluid dynamics (CFD) simulations that solve for the flow through the building can overcome these limitations, and are increasingly used in the study of air circulation in buildings. CFD simulations can be shown to provide improved accuracy, but they do require significantly larger computational times, and they represent a level of detail in the building model that is unlikely to be well defined in early design stages. This implies that, despite their limited accuracy, box models can be very useful to guide early design decisions, while CFD models can provide the necessary accuracy for optimizing final design choices.

In the present study we investigate the predictive capability of a box model and a CFD simulation for determining the night-flush ventilation efficiency in the Y2E2 building on Stanford's campus. The Y2E2 building is a 3-floor building in which the hallways and common areas are cooled by natural (night-flush) ventilation through 4 separate atria. The models presented in this paper consider a single atrium, and the predictions will be compared to temperature measurements available on each floor of the

atrium. The results presented were obtained for the first 4 hours of the night flush on August 3rd 2010, when the windows of the upper two floors of the atrium were open. The objective of the study is threefold: 1. To compare the air temperature predicted by the box model and CFD model to the measurements, 2. To rank the importance of the different uncertain input parameters in the box model in terms of their impact on the model results, and 3. To use CFD simulation results for investigating the box model assumptions. In the present paper we first perform an uncertainty quantification (UQ) study for the box model to determine the influence of the different model parameters and subsequently we perform CFD simulations to investigate whether a more accurate result is obtained and to extract the heat transfer coefficient and discharge coefficient used in the box model from the CFD results.

The remainder of this paper is organized as follows. Section 2 presents the Y2E2 building configuration, the night-flush operational details and the available measurements. Section 3 presents modeling details of the box model, while section 4 discusses the set-up of the CFD model. Section 5 includes the results obtained using both models and in Section 6 conclusions and future work are summarized.

2 Y2E2 NATURAL VENTILATION SYSTEM AND AVAILABLE MEASUREMENTS

The Yang and Yamazaki Environment and Energy Building (Y2E2) has 14,000m^2 of floor space on three above ground levels and one basement level. The building uses a combination of passive and active heating, cooling and ventilation systems. It has four atria and exposed concrete slab floors in almost all rooms and common spaces to provide thermal mass for the natural ventilation system. In the present operation of the building a night flush is used to cool common spaces (hallways, open areas and lounges connected to the central atria) during summer nights. Cool air enters through mechanically operated windows on the 1st through 3rd floors and exits through mechanically operated louvers at the top of each atrium. The night flush cycle starts at 7pm, on the condition that the outdoor temperature, T_o, is lower than the indoor air temperature $T_{a,j}$, where j is the floor level (1, 2 or 3). Additionally, the indoor temperature $T_{a,j}$ must be greater than 295.5K at the start of the flush. The windows on each floor are controlled separately and $T_{a,j}$ is the mean temperature from the sensors in each of the 4 atria on floor j. If the temperature on a given floor cools to 293.5K during the night flush, the windows close and remain closed until the temperature exceeds the 295.5K limit again. The modeling effort presented in this paper focuses on the night flush in Atrium D during the night of August 3rd 2010. Figure 1 plots the temperature measurements on each floor and averaged over all floors, and the outdoor temperature from 8pm on August 3rd till 5am on August 4rth. When the temperature is plotted as a solid thick line, the windows on the corresponding floor were open and an active night flush occurred. The thin vertical dashed line indicates the end time of the active nightflush, which lasted 4 hours, and the result presented in this paper will focus on these 4 hours. The plot shows that when the windows are opened the temperature drops immediately, with the fastest decrease in temperature observed on the top floor. Within one hour the temperature on the third floor decreases by 1K to the level of the first floor where the windows remained closed. After 4 hours the temperature has dropped below the threshold on both the second and the third floor and the windows are closed. Once the windows close the temperature on the third floor starts to increase again, while the other two floors continue to cool down, returning the atrium to a stably stratified condition. When the outdoor temperature starts to rise again the indoor temperature on each floor follows that trend. The measurements demonstrate that the 3.7K decrease in outdoor air temperature during the period of the nightflush provides sufficient natural ventilation cooling potential to ensure the indoor temperature conforms with the design conditions.

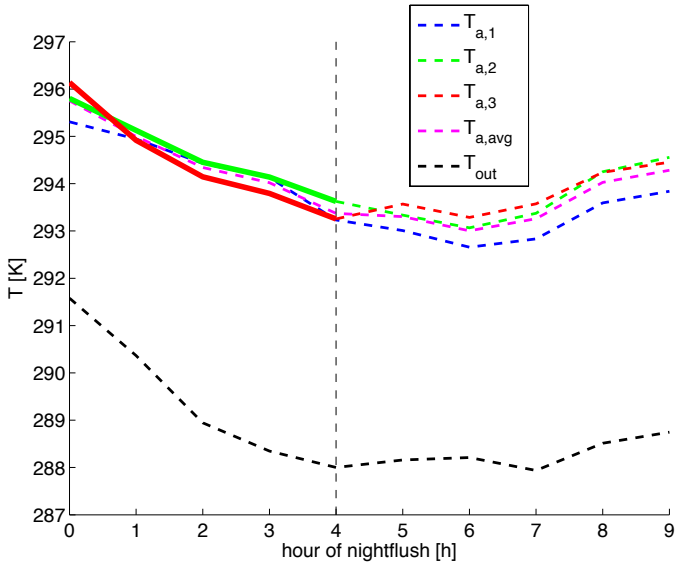

Figure 1. Measured outdoor and indoor (floor 1, 2, 3 and average) air temperature during the nightflush of 08/03/2010. Solid thick lines indicate that the windows on the second and third floor were opened during the first four hours of the nightflush.

3 NIGHT-FLUSH BOX MODEL EQUATIONS

3.1 Governing Equations for Air and Thermal Mass Temperature

The box model solves for the evolution of the average temperature of the indoor air T_a and building thermal mass T_{tm} over time. The governing equations are given by:

$$V_a \rho_a c_{p,a} \frac{dT_a}{dt} = -q_{nv} - q_{in} - q_e + q_i + q_{conv} \quad (1)$$

$$\sum_{i=1}^{M} \left(A_{tm,i} t_{tm,i} \rho_{tm,i} c_{p,tm,i}\right) \frac{dT_{tm}}{dt} = -q_{conv} \quad (2)$$

V_a, ρ_a and $c_{p,a}$ are the volume, density and specific heat of the air. q_{nv} is the heat loss through natural ventilation, q_{in}, is the heat loss through infiltration, q_e is the heat flux through the building envelope, q_i is the internal load and q_{conv} is the convective heat transfer between the air and the thermal mass. The thermal mass consists of all concrete floors and gypsum ceilings, and $A_{tm,i}$, $t_{tm,i}$, $\rho_{tm,i}$ and $c_{p,tm,i}$ are the respective area, thickness, density and specific heat for these thermal masses. While the different surfaces have a different thermal response, radiation heat exchange will act to bring surfaces to similar temperatures [1] and the model therefore assumes that the different thermal masses are at the same temperature. Table 1 presents the values used for the air and thermal mass properties, and the following subsections summarize how the different right hand side terms in the equations are modeled and what the uncertainty in the representation of the different terms is.

Table 1. Geometrical characteristics and properties of air and thermal mass.

	Air	Thermal mass	
		Concrete Floors	Gypsum Ceilings
Volume [m^3]	2880	-	-
Area [m^2]	-	600	600
Thickness [m]	-	0.1	0.025
Density [kg/m^3]	1.225	2300	2320
Specific heat [J/kg-K]	1006.43	750	1132

3.2 Convective Heat Transfer

Convective heat transfer is modeled as:

$$q_{conv} = h \sum_{i=1}^{M} \left(A_{tm}\right) \left(T_{tm} - T_a\right) \quad (3)$$

using a single constant heat transfer coefficient h between the air and the different thermal masses. In a previous study [2] the heat transfer coefficient was specified as 1.75W/m^2K. The uncertainty in this value is considerable, given that h is a time and space dependent variable, and values between 1 and 4 W/m^2K could realistically occur. This range was therefore used for the initial UQ study. Subsequently the CFD simulation results will be used to calculate whether the heat transfer coefficient is within this range.

3.3 Natural Ventilation Heat Loss

The heat loss because of natural ventilation is defined as:

$$q_{nv} = \rho_a c_{p,a} \dot{V}_{nv} \left(T_a - T_{out}\right) \quad (4)$$

where the total flow rate is approximated as the sum of the airflow through the different windows based on Bernoulli's equation:

$$\dot{V}_{nv} = C_{d,0} \sum_{w=1}^{W} A_w \left(2 g H_w \frac{T_a - T_{out}}{T_a}\right)^{1/2} \quad (5)$$

with A_w the effective area of the different inlet windows, g the gravitational acceleration, and H_w the height difference between the inlet and outlet. The geometry of the outlet vents with mechanically operated louvres does not affect the ventilation flow rate, since their area is much larger than that of the inlet windows. Table 2 summarizes the geometrical characteristics of the different inlet windows. During the night flush considered the windows on the second and third floor were opened with an angle between 38 and 46°. $C_{d,0}$ is the effective drag coefficient for the modeled configuration and is a function of the window opening angle. In [2] detailed CFD simulations of representative window openings at different angles were performed to determine the effective drag coefficient, and for an angle of 42° a value of 0.48 was found. Despite this detailed study it should be expected that the actual value of $C_{d,0}$ can deviate from 0.48, since a) the exact opening angle is unknown, b) in reality $C_{d,0}$ is a time dependent property and c) the configuration in which the window is implemented differs from the idealized CFD model used in [2]. The box model UQ study will be performed using a value between 0.42 and0.58 [2]. Based on the CFD simulations an updated value will be calculated for each floor separately, i.e. in eq. 5 a discharge coefficient is specified for each window inside the sum.

Table 2. Geometrical characteristics of the inlet windows.

	First Floor	Second Floor	Third Floor
Area [m^2]	1.57	1.83	1.83
Stack Height [m]	11.35	6.62	2.07
Angle [^{o}]	0	38-46	38-46

3.4 Infiltration Heat Loss

Infiltration is unintended airflow through e.g. cracks and unclosed windows or doors. The effective infiltration depends on the construction of the building and on environmental parameters and is difficult to measure or estimate. In [2] the infiltration flow rate was estimated by fitting box model results to observations on a night where the windows remained closed, i.e. when no night flush occurred. The resulting infiltration flow rate is added to the model in the form of Eq. (5) using a window with an effective area of 0.55m^2 at the mean stack height (6.68m) of the building. This simplified representation of the infiltration heat loss and the fitting procedure used to determine the additional effective window area imply that q_i is an additional uncertainty. In the present study it is assumed to be between 0.1m^2 and 1.5m^2.

3.5 Heat Flux Through Building Envelope

The walls of the atrium are either internal walls that are adjacent to offices, or external walls. Offices on the south and west side are climate controlled, and might remain cooler than the common atrium space during the day, but at night the cooling system is shut down and temperature differences are likely to be small. Offices on the north and east side rely solely on natural ventilation for cooling and are expected to be at similar temperatures as the atrium. As a result, the internal walls are considered to be adiabatic in the present study. The heat exchange through the external walls is modeled using a thermal resistance formulation:

$$q_e = \frac{A_{w,ext}}{R_{w,ext}} (T_a - T_{out}) \tag{6}$$

where $A_{w,ext}$ is the external wall area equal to 184m^2, and $R_{w,ext}$ is the overall thermal resistance of 2.72m^2K/W. It is noted that the model assumes that heat exchange with the outdoors does not directly affect the temperature of the thermal mass, but in reality wall heat exchange could lead to a temperature gradient within the thermal mass. In the present study, the uncertainty in the heat exchange through the building envelope is represented by a 25% uncertainty in the value of $R_{w,ext}$.

3.6 Internal Loads

As in [2], the internal load estimates for the space are taken from the energy analysis done by ARUP. This analysis specified occupant, lighting and equipment loads for each interior zone of the building. For most zones in the atrium the peak occupant load is 5.4W/m^2, the peak lighting load is 10.8W/m^2 and the peak equipment load is 7.5W/m^2. During the night flush the actual loads are only a fraction of these peak loads, and Figure 2 presents the resulting total internal load in W/m^2 for each hour of the nightflush. These loads are estimates based on predictions for user behavior and have an uncertainty associated to them, which in the present study was assumed to be 50%.

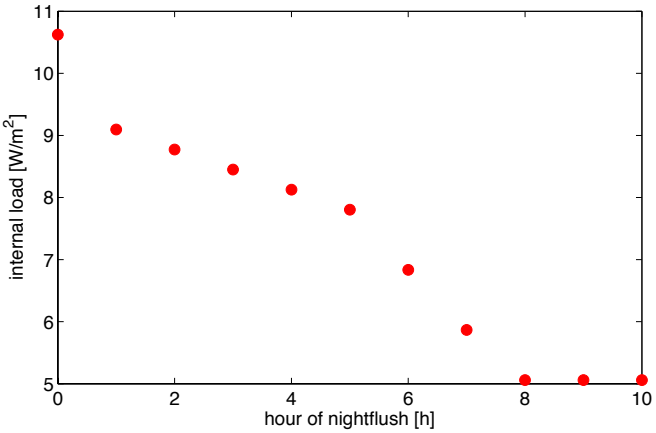

Figure 2. Internal heat load estimate for a weekday evening night flush.

3.7 Initial and Boundary Conditions, Solution Method and Uncertainty Propagation

The outdoor temperature is specified as a function of time using the available outdoor temperature measurement (see Figure 1). The initial temperature of the indoor air was equal to 295.75K, which corresponds to the value measured right before the opening of the windows. The initial thermal mass temperature is treated as an uncertain parameter, with the maximum value

equal to the initial air temperature of 295.75K, and the minimum value 2K lower, i.e. 293.75K. The resulting equations are solved using an explicit Euler method with a time step of 15s.

In total 6 uncertain variables have been identified in the box model. Table 3 provides an overview of these variables and their assumed minimum and maximum values. For the internal loads the minimum and maximum of the time series are presented. In this initial study uniform distributions were assumed for all uncertain input variables. A non-intrusive polynomial chaos approach was used to propagate the input uncertainties through the boxmodel and quantify their effect on the output. The chaos coefficients were computed using Clenshaw Curtis quadrature on an isotropic tensor grid [3,4] with 5 points in each uncertain direction, resulting in a total of 15625 box model evaluations. The quantities of interest were the air and thermal mass temperature at 15 minute intervals during the 4 hour nightflush cycle, resulting an a total of 34 quantities if interest. For each quantity of interest the mean and variance was computed, and 95% confidence intervals were obtained by constructing probability distributions of PCE response surface evaluations for 50000 samples drawn from the uncertain input space.

Table 3. Uncertain box model parameters.

	Minimum	Maximum
Heat transfer coefficient h [W/m^{2}K]	1.0	4.0
Discharge coefficient $C_{d,0}$ [-]	0.42	0.58
Effective window area for infiltration [m^2]	0.1	1.5
External wall resistance [m^{2}K/W]	2.04	3.4
Internal loads [W/m^2]	4.0 - 5.2	12.0 - 15.7
Initial thermal mass temperature [K]	293.75	295.75

4 NIGHT-FLUSH CFD MODEL

4.1 Governing Equations and Solution Method

Fluent v15 was used to solve the incompressible unsteady Reynolds-averaged Navier-Stokes equations. The effect of buoyancy is represented using the Boussinesq model, where density is treated as a constant value in all solved equations, except for the buoyancy term in the momentum equation which is modeled as:

$$(\rho - \rho_0)\, g \approx -\rho_0 \beta\, (T - T_0)\, g \tag{7}$$

where ρ_0 is the constant density of the flow, T and T_0 the local and reference temperature respectively, and β the thermal expansion coefficient of the fluid. This approximation is valid as long as the actual density variations in the flow are small, which is the case in the present simulations. The resulting equations for conservation of mass, momentum and energy are:

$$\frac{\partial \overline{U_i}}{\partial x_i} = 0 \tag{8}$$

$$\frac{\partial \overline{U}_j}{\partial t} + \overline{U_i}\frac{\partial \overline{U}_j}{\partial x_i} = -\frac{1}{\rho_0}\frac{\partial \overline{p}}{\partial x_j} + \frac{\mu}{\rho_0}\frac{\partial^2 \overline{U_j}}{\partial x_i \partial x_i} - \frac{\partial \overline{u_i u_j}}{\partial x_i} - \beta\,(T - T_0)\, g_j \tag{9}$$

$$\frac{\partial}{\partial t}(E) + \frac{\partial}{\partial x_i}\left(u_i\left(E + \frac{p}{\rho_0}\right)\right) = \frac{K}{\rho_0}\frac{\partial^2 T}{\partial x_i \partial x_i} + S_h \tag{10}$$

Turbulence is modeled with the Renormalizaton Group Theory (RNG) k-ε turbulence model. In several studies this model has been recommended for indoor airflow simulations [5,6].

The PISO scheme is used for the pressure velocity coupling, and the discretization schemes for all variables are 2nd order. Time discretization is done using a first order implicit scheme with a time step of 15s and a maximum of 20 iterations per time step.

4.2 Computational Domain, Mesh, and Boundary Conditions

The building model is shown in Figure 3 and represents one atrium that consists of the three floors and the upper section of the atrium with the flow outlets. The computational mesh was generated using the Fluent meshing tool and consists of 1.1 million cells. The resolution near the windows results in at least 10 cells along each window edge and is gradually increased when moving away from the windows with a maximum of 32cm. In addition to the building geometry shown in Figure 3, the model includes 4 volumes on the outside of the building adjacent to the inlet windows and top outlets, such that pressure and temperature boundary conditions can be specified outside of the building geometry. The pressure on these boundaries is specified as a constant value, while the temperature follows the profile measured during the night of interest as shown in Figure 1.

On the window openings between the outdoor and indoor fluid domain a porous jump condition is applied to represent the additional pressure drop that occurs because the windows are opened at a 38^o to 46^o angle. The porous jump condition specifies the additional pressure loss as:

$$\Delta p = -C2\frac{1}{2}\rho U^2 \tag{11}$$

where C_2 is equal to 1.65. This value was determined based on the discharge coefficients calculated in [2] to correct the pressure drop of a fully open window to the value of a window at a 42° angle. The sidewall boundaries are specified as adiabatic no-slip boundaries, both for internal and external walls. On the floor and the ceilings a temperature boundary condition that represents the evolution of the thermal mass temperature with a user-defined function is specified. Section 4.3 discusses and justifies this approach in more detail. The heat flux through the building envelope is not represented in the model, this assumption is justified based on the limited influence of this parameter as observed in the box model (see Section 5.1). A volumetric source term is specified inside the building to represent the internal heat load, following the profile shown in Figure 2.

The initial conditions are defined based on the building measurements shown in Figure 1, i.e. the temperatures measured on the different floors and outside of the building are imposed in the corresponding volumes of the CFD model. The initial temperature of the thermal mass is assumed to be equal to the average indoor air temperature. To investigate the influence of this assumption, an additional simulation where the initial thermal mass temperature was 1.5K lower than the air temperature was performed. The temperature difference between the outdoor and indoor air initiates a buoyancy driven flow pattern at the start of the simulation.

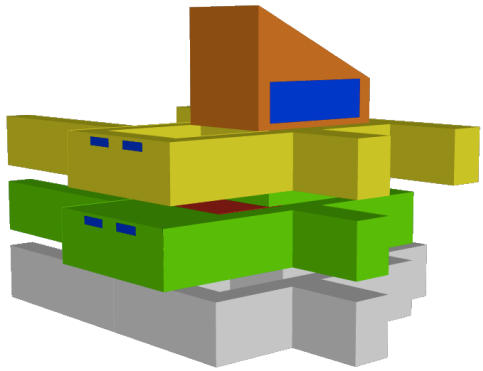

Figure 3. Single atrium geometry without explicit modeling of the thermal mass.

4.3 Thermal mass modeling

The most complete approach for modeling the interaction between the air and the thermal mass is to solve a conjugate heat transfer problem where both the fluid and solid volumes in the computational domain are represented. This enables calculating the local temperature in the thermal mass and the heat transfer at the interface between the thermal mass and the air. Since this approach increases the complexity of the set-up of the computational model an alternative approach was explored as well, where the thermal mass is considered to have one uniform temperature, and the variation of this volume-averaged temperature over time as a result of convective heat transfer is represented using a user-defined-function (udf) at the floor and ceiling wall boundaries. The udf updates the thermal mass temperature at every time step:

$$T_{tm(t+1)} = T_{tm(t)} + dt * \sum_{i=1}^{TM} \frac{q_{conv(i,t)}}{A_{tm(i)} t_{tm(i)} \rho_{tm(i)} c_{p,tm(i)}} \tag{12}$$

where T_{tm} is the volume-averaged temperature of the thermal mass, dt the time step, TM the total number of surfaces where convective heat transfer between the air and the thermal mass occurs, $q_{conv(i,t)}$ the integral convective heat flux on each surface at every time step, and $A_{tm(i)}$, $t_{tm(i)}$, $\rho_{tm(i)}$ and $c_{p,tm(i)}$ the area, thickness, density and specific heat capacity corresponding to each thermal mass interface. The effect of using this udf was investigated on the simplified atrium geometry shown in Figure 4(a), by comparing full conjugate model results to the results obtained with the udf. The model consists of three floors with one window on each floor, and an outlet at the top of the atrium located on the backside of the view provided in Figure 4(a). Similar to the detailed atrium model, the computational domain also includes 4 small outdoor air volumes on the outside of each window (not shown in Figure 4(a)). Figure 4(b) shows the boundary condition imposed for the outdoor temperature evolution for this case.. In this test case no internal heat load was imposed, and, similar to the detailed atrium CFD model, heat exchange through the building envelope is assumed to be negligible.

Figure 5 presents contours of the temperature through the center of the simplified atrium geometry at 2 hour intervals during the nightflush. Locally small temperature differences can be observed, but the volume-averaged thermal mass and air temperatures differ by less than 0.5K throughout the night. This indicates that the volume-averaged representation of the thermal mass is sufficiently accurate to model the nightflush in the full atrium and extract values of the heat transfer coefficient and discharge coefficient.

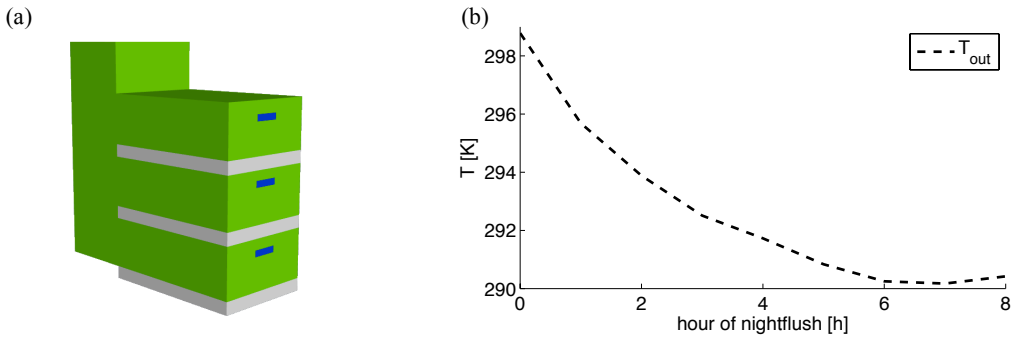

Figure 4. (a) Simplified atrium geometry to investigate the effect of the representation of the thermal mass, (b) Outdoor temperature profile

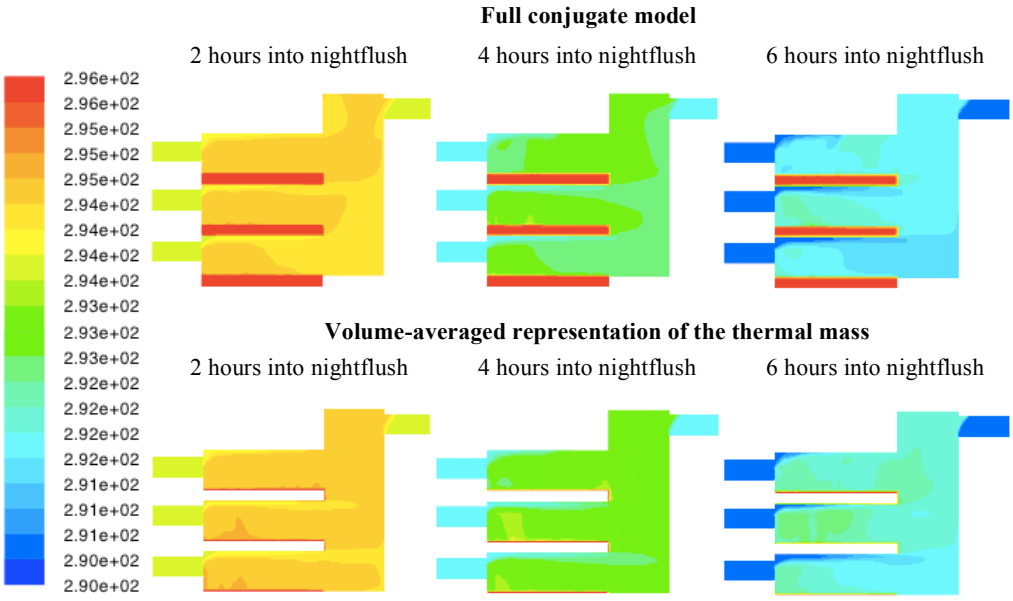

Figure 5. Temperature contours showing the difference between the temperature evolution in the full conjugate model and the model with a volume-averaged representation of the thermal mass

5 RESULTS

In the following sections we first present the results of the box model UQ study to investigate the influence of uncertainty in the box model input parameters on the predicted air and thermal mass temperature evolution. Subsequently the temperature evolutions obtained from the CFD simulations are compared to the experimental data and used to calculate the heat transfer and discharge coefficients.

5.1 Box model UQ study

Figure 6 presents the mean and 95% confidence interval (CI) for the air and thermal mass temperature as a function of time, where the confidence interval has been computed from 50000 evaluations of the PCE response surface. The average measured air and thermal mass temperature is also included for comparison. The plot shows that the measured air temperature is within the 95%CI, and that the mean box model result predicts a too fast cooling rate. The maximum discrepancy between the mean box model and the measured data is 0.6K during the 4 hour nightflush. The magnitude of the 95%CI for the air temperature slowly increases over time, with a maximum interval of 2.5K at the end of the nightflush. The 95%CI interval for the thermal mass temperature shows a very small decrease from 1.8K to 1.4K and is clearly governed by the input range To understand which parameters contribute most to the variance of the output, Figure 7 plots the Sobol Indices for the air and thermal mass temperatures during the nightflush. The plot illustrates that during the first 2 hours the main contribution to the variance is from the effective window area for infiltration, the initial thermal mass temperature and the internal heat source. During the second half of the nightflush the last two become less important, and the heat transfer coefficient has a more significant contribution. For the thermal mass temperature the initial temperature governs the variance throughout the night.

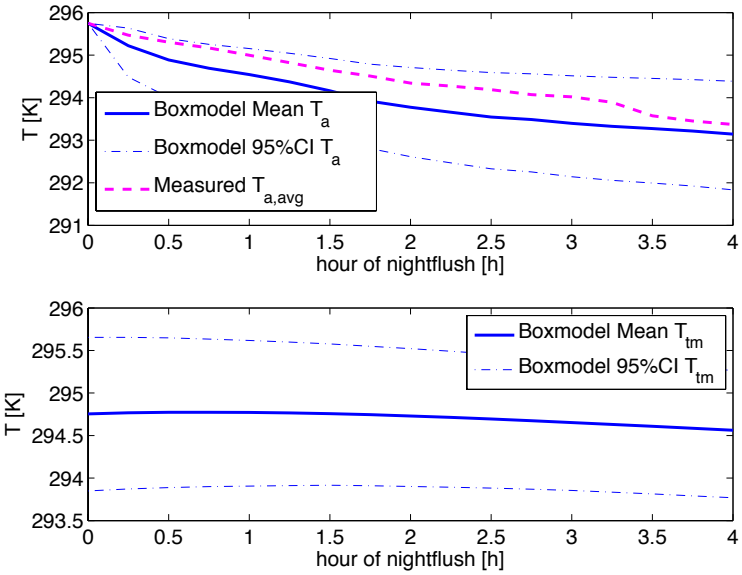

Figure 6. Mean and 95%CI for the air and thermal mass temperature obtained from the box model UQ study and comparison to measured air temperature

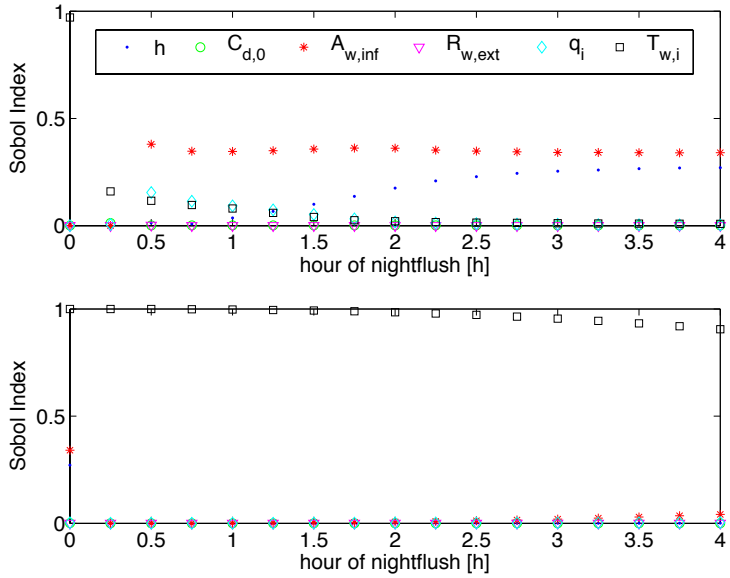

Figure 7. Sobol indices for the different uncertain parameter

5.2 CFD results

Figure 8 shows the predicted air temperature as a function of time for both CFD simulations, i.e. one where the initial thermal mass temperature is equal to the air temperature, and one where it is 1.5K lower. The difference between both simulations is negligible, and similar to the box model, a slightly too high cooling rate is obtained. The maximum discrepancy between the average air temperature from the CFD model and the measurement is 0.9K, which is comparable to the discrepancy observed between the mean box model and the measurement. When comparing the temperature on each floor separately the largest discrepancy occurs on the second floor and is equal to 1.6K.

Figure 9 shows the mass flow rate through the window openings on the different floors and the corresponding discharge coefficients for both simulations, indicating that the initial thermal mass temperature has a negligible influence on the flow rate. The mass flow on the first floor is zero since the windows remained closed. The second floor has the highest mass flow rate, which can be explained by the higher effective stack height and by the internal building geometry. The effect of the difference in stack height is explicitly represented in Eq. 5, but the internal geometrical differences have to be accounted for by the discharge coefficient. Consequently, the discharge coefficients on the second floor are higher than those on the third floor, with an average value of 0.63 (0.59 for the lower initial thermal mass temperature) and 0.22 (or 0.21 for the lower initial thermal mass

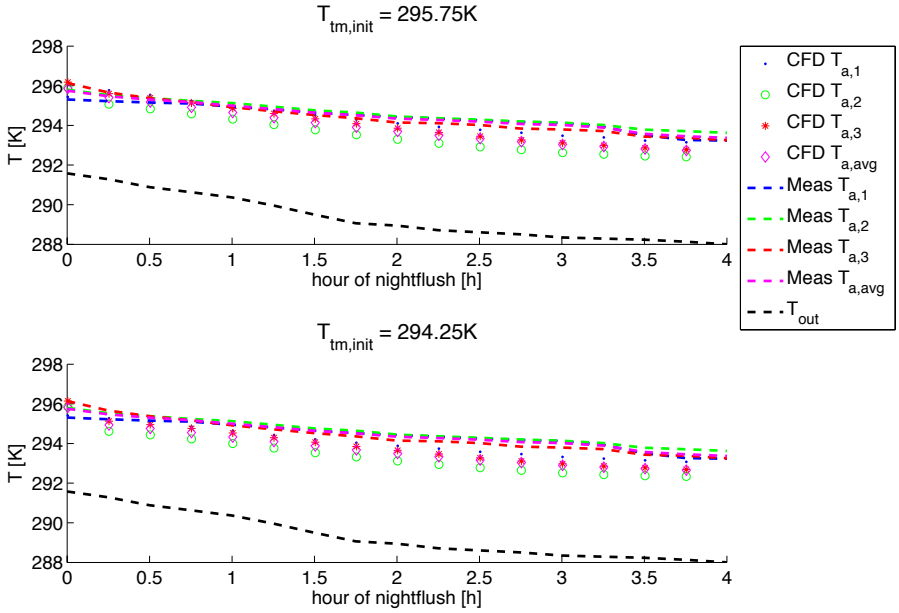

Figure 8. CFD prediction for the evolution of the air temperature and comparison to the measured data

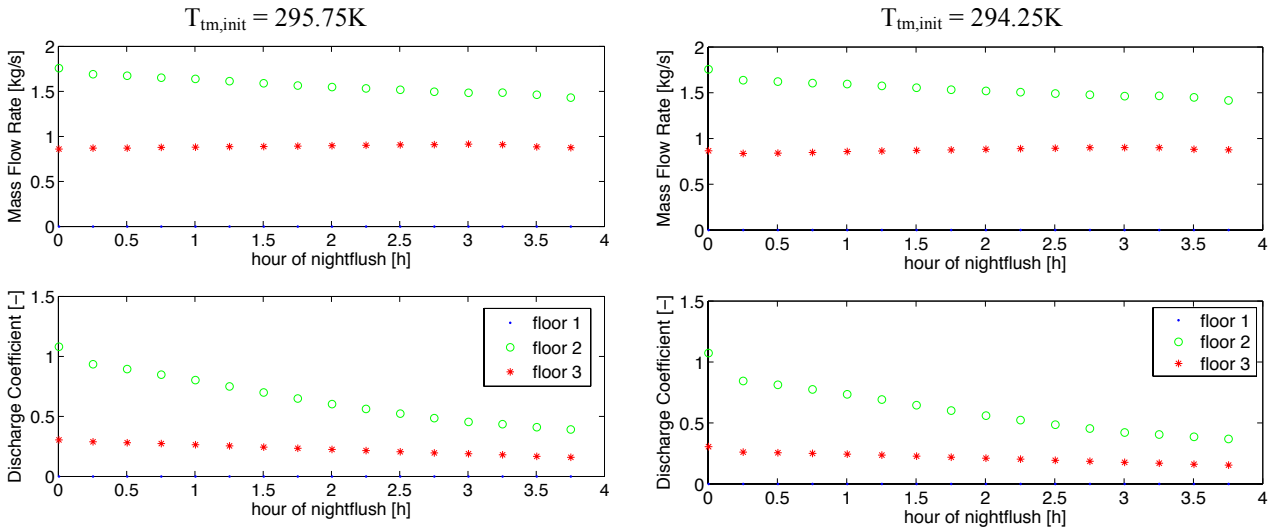

Figure 9. Mass flow rates and corresponding discharge coefficients through the window openings on the different floors

temperature) respectively. The values also vary strongly over time, with a maximum of 1.1 and a minimum of 0.35 on the second floor and a maximum of 0.31 and a minimum of 0.15 on the third floor. These values are outside of the range considered in the box model UQ study, which will be taken into account in future work.

Figure 10 shows the integrated surface heat flux on all ceilings and floors and the corresponding heat transfer coefficient. It is shown that the initial thermal mass temperature has a significant effect on the integrated surface heat flux and on the initial values of the heat transfer coefficient, but after 1.25 to 1.5 hours a heat transfer coefficient of ~2.9 W/m^{2}K is obtained in both simulations. This value slowly decreases to ~2.7 W/m^{2}K at the end of the nightflush. The average value for the heat transfer coefficient is 2.79 W/m^{2}K for the simulation with the higher initial thermal mass temperature and 2.86 W/m^{2}K for the one with the lower initial thermal mass temperature, which is within the range considered in the box model UQ study.

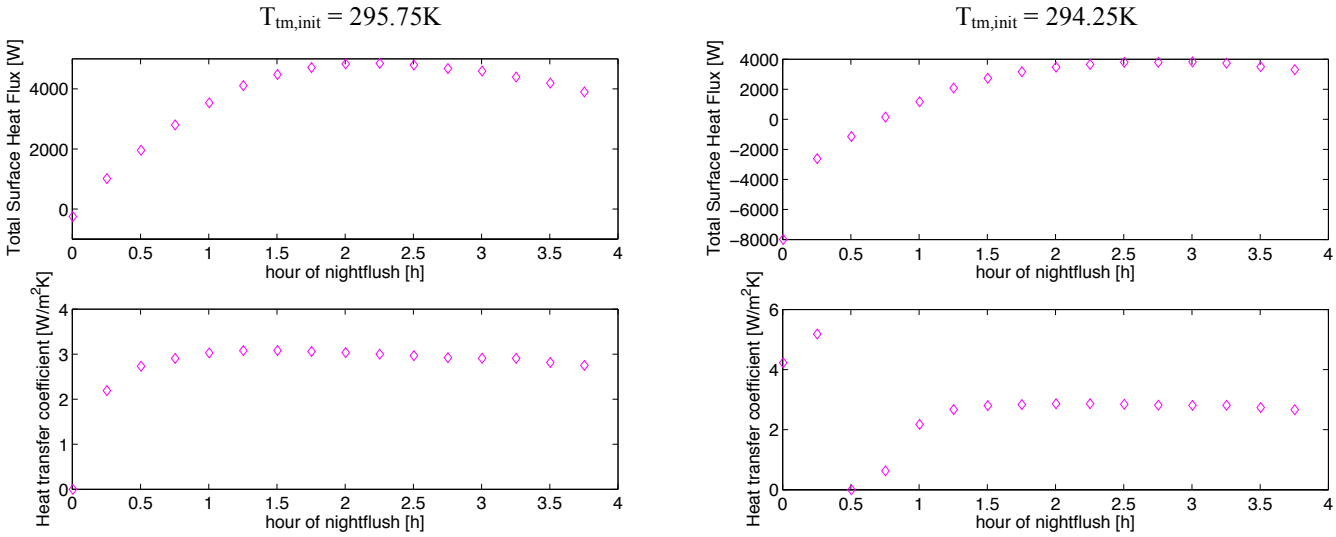

Figure 10. Mass flow rates and corresponding discharge coefficients through the window openings on the different floors

6 CONCLUSIONS AND FUTURE WORK

An important fraction of the energy consumption in buildings is related to controlling the indoor temperature through heating, ventilating or air conditioning. In moderate to cold climates passive cooling by nighttime ventilation could result in significant energy savings, but the design and performance prediction of a natural ventilation system remains a challenging task.

In the present study we investigated the predictive capability of a box model and a CFD simulation for determining the night-flush ventilation efficiency in the Y2E2 building on Stanford's campus. The models have a very different level of detail in the representation of the building and the natural ventilation physics and both consider a single atrium of the Y2E2 building. The predictions have been compared to temperature measurements available in that atrium.

The box model solves for the average temperature of the air and the building thermal mass, and represents heat sources and sinks using integral values. There is significant uncertainty in the definition of the input parameters required by the box model, and the uncertainty in these inputs was propagated to the output using a non-intrusive polynomial chaos method. It was found that the average measured building temperature is within the 95%CI predicted by the model. The mean box model result was shown to predict a slightly too fast cooling rate, but the maximum discrepancy between the mean box model and the measured data during the 4 hour nightflush is only 0.6K. During the first 2 hours the main uncertainty in the result for the air temperature is related to the uncertainty in the effective window area for infiltration, in the initial thermal mass temperature and in the internal heat source. During the second half of the nightflush the last two become less important, and the heat transfer coefficient has a more significant contribution. For the thermal mass temperature the initial temperature governs the variance throughout the night.

The CFD simulation represents a much higher level of detail in the building model and solves for the flow and heat transfer through the building. Two simulations were performed to investigate the influence of different initial conditions for the thermal mass temperature, and it was shown that the effect on the average air temperature is small. In both CFD simulations the maximum discrepancy between the average air temperature from the CFD model and the measurement was found to be 0.9K, which is comparable to the discrepancy observed between the mean box model and the measurement. The results of the CFD simulations were also used to verify the values used for discharge and heat transfer coefficients in the box model. The discharge coefficients computed from the CFD simulation are different for each floor and have a strong dependency on time. The values vary from 1.1 to 0.15, and have a mean value that is outside of the range originally assumed in the box model UQ study. The heat transfer coefficient depends on the initial thermal mass temperature during the first 1.5 hours of the nightflush, but eventually the value converges to around 2.7 W/m^2K, which is within the range computed by the box model.

Future work will focus on additional CFD simulations to understand why a too high cooling rate is predicted, and on developing multi-fidelity simulation strategies where information from the box model and the CFD model are optimally used for design and performance prediction of natural ventilation systems.

ACKNOWLEDGMENTS

This project was supported by seed funding from the Precourt Energy Efficiency Center at Stanford University. The authors acknowledge previous work on modeling natural ventilation in the Y2E2 building by Erin Hult [2], which provided an invaluable starting point for the present study.

REFERENCES

[1] M.A. Menchaca-Brandan and L.R. Glicksman. The importance of accounting for radiative heat transfer in room airflow simulations. RoomVent 2011 Procdeedings, 2011.
[2] E. Hult, G. Iaccarino and M. Fischer. Simulation of night purge ventilation using CFD and airflow network models. Stanford Internal Report, 2011.
[3] G. Iaccarino. Introduction to uncertainty representation and propagation. AVT-193 short course on uncertainty quantification, 2011.
[4] M.S. Eldred and J. Burckardt. Comparison of non-intrusive polynomial chaos and stochastic collocation methods for uncertainty quantification, AIAA Paper, 2009-0976.
[5] Q. Chen. Comparison of different k-e models for indoor air flow computations. Numerical Heat Transfer Part B Fundamentals, 28(3):353-369, 1995.
[6] Y. Ji, M.J. Cook, and V. Hanby. CFD modeling of natural displacement ventilation in an enclosure connected to an atrium. Building and Environment, 42(3):1158:1172, 2007.